

*Annals of Neurology, in press*

**Amyloid- $\beta$  Associated Cortical Thinning in Clinically Normal Elderly**

J. Alex Becker, PhD<sup>1</sup>, T. Hedden, PhD<sup>2,8</sup>, J. Carmasin, BS<sup>1</sup>, J. Maye, BS<sup>1</sup>, D.M. Rentz, PsyD<sup>3,4</sup>, D. Putcha, BA<sup>2</sup>, B. Fischl, PhD<sup>1,2</sup>, D. Greve, PhD<sup>1,2</sup>, G. Marshall, MD<sup>3,4</sup>, S. Salloway, MD<sup>5,6</sup>, D. Marks, MD<sup>7</sup>, R.L. Buckner, PhD<sup>1,2,8,9,10</sup>, R.A. Sperling, MD<sup>3,4</sup> and K.A. Johnson, MD<sup>1,3,4</sup>

<sup>1</sup>Department of Radiology, Massachusetts General Hospital, Harvard Medical School

<sup>2</sup>Athinioula A. Martinos Center for Biomedical Imaging

<sup>3</sup>Department of Neurology, Brigham and Women's Hospital, Harvard Medical School

<sup>4</sup>Department of Neurology, Massachusetts General Hospital, Harvard Medical School

<sup>5</sup>Department of Neurology, Warren Alpert Medical School, Brown University

<sup>6</sup>Memory and Aging Program, Butler University

<sup>7</sup>Tufts School of Medicine

<sup>8</sup>Department of Psychology and Center for Brain Science, Harvard University

<sup>9</sup>Department of Psychiatry, Massachusetts General Hospital and Harvard Medical School

<sup>10</sup>Howard Hughes Medical Institute

**Running Title: A $\beta$  and cortical thinning in normal aging**

Title: 60 Characters (not including spaces)

Running Head: 34 Characters (not including spaces)

Abstract: 181 words

Text: 4606 words

References: 76 refs

Number of Figures: 3 (1 Color)

Number of Tables: 2

**Corresponding Author:**

Keith A. Johnson, M.D.

## **Abstract:**

**Introduction:** Both amyloid- $\beta$  ( $A\beta$ ) deposition and brain atrophy are invariably associated with Alzheimer's disease (AD) and the disease process likely begins many years before symptoms appear.

**Objective:** We sought to determine whether clinically normal (CN) older individuals with  $A\beta$  deposition revealed by PET imaging using Pittsburgh Compound B (PiB) also have evidence of both cortical thickness and hippocampal volume reductions in a pattern similar to that seen in AD.

**Methods:** One hundred and nineteen older individuals (87 CN subjects and 32 patients with mild AD) underwent PiB PET and high-resolution structural MR. Regression models were used to relate PiB retention to cortical thickness and hippocampal volume.

**Results:** We found that PiB retention in CN subjects was (1) age-related and (2) associated with cortical thickness reductions particularly in parietal and posterior cingulate regions extending into the precuneus, in a pattern similar to that observed in mild AD. Hippocampal volume reduction was variably related to  $A\beta$  deposition.

**Interpretation:** We conclude that  $A\beta$  deposition is associated with a pattern of cortical thickness reduction consistent with AD prior to the development of cognitive impairment.

Study supported by: NIH/NIA; Massachusetts ADRC; Alzheimer's Association; HHMI; Anonymous Foundation

## **Introduction:**

The possibility of disease-modifying therapies for Alzheimer's disease (AD) has motivated the development of biomarkers that reflect underlying pathologic processes. The sequence of pathologic events in AD likely begins many years, perhaps decades, prior to the development of symptoms<sup>1,2</sup>. A $\beta$  deposition appears early in the disease, prior to symptoms, and then plateaus as clinical dementia emerges<sup>3-6</sup>. In contrast, neurodegeneration, including loss of synapses, neurons and arborization, results in brain atrophy that worsens inexorably in parallel with cognitive decline<sup>2,6,7</sup>. The principal early sites of A $\beta$  deposition are neocortical, typically parietal and frontal regions<sup>4,8,9</sup>, whereas the sites of early atrophy include medial temporal regions<sup>2,6,10,11</sup>. Here we relate these two phenomena *in vivo* in clinically normal older individuals and in clinically established AD patients, in order to determine the correspondence between levels of A $\beta$  deposition and of atrophy.

It is now possible to observe the relation between A $\beta$  deposition and atrophy *in vivo* with PET imaging using Pittsburgh Compound B (PiB)<sup>9</sup> and high resolution volumetric MR data<sup>2,12</sup>. PiB studies have confirmed what was predicted by earlier postmortem studies<sup>13-15</sup>, that a substantial fraction (25-50%) of clinically normal older individuals exhibit A $\beta$  deposition<sup>16-21</sup>. While still in an early phase, PET studies of A $\beta$  deposition in these otherwise normal individuals suggest evidence of early brain dysfunction including disrupted default network functional connectivity<sup>19,21</sup>, aberrant default network activity during memory encoding<sup>18</sup>, and even subtle cognitive impairment<sup>22,23</sup> that is offset by cognitive reserve<sup>23</sup>. Here we relate the presence and pattern of A $\beta$ -related atrophy observed in AD patients to the pattern seen in clinically normal older individuals.

Atrophy can be quantified by automated measurement of brain MR images, which yields estimated thickness measures of anatomically parcellated cortical regions as well as subcortical volumes<sup>24-27</sup>. Such measurements have revealed a characteristic pattern of cortical thickness reductions

and subcortical volume loss in clinically diagnosed AD patients<sup>25, 27-29</sup>. The AD-like pattern of atrophy has also been reported in presymptomatic autosomal dominant AD<sup>28</sup>, and in those with mild cognitive impairment who go on to develop the clinical diagnosis of AD<sup>30</sup>. More recently, Desikan et al.<sup>11</sup> identified a pattern of atrophy in supramarginal cortex, entorhinal cortex, and hippocampus with which MCI and AD could be distinguished from normal aging, and Davatzikos et al. identified a similar pattern of volume loss that related to cognitive decline among MCI as well as normal control subjects<sup>31, 32</sup>. However, these studies used control groups of older individuals in which amyloid was likely present, but the impact was not assessed. Studies directly relating structural data to A $\beta$  deposition in CN subjects have yielded inconsistent results; while some have reported reduced hippocampal volume<sup>33, 34</sup> or cortical thickness<sup>29, 34</sup> in CN subjects with greater A $\beta$  deposition, others have found this only among A $\beta$ -positive CN<sup>35</sup> or in normal individuals with subjective cognitive impairment<sup>36</sup>. Similarly, the impact of age on amyloid and atrophy has not been consistently controlled. We sought to relate both hippocampal volume and cortical thickness reductions to a continuous measure of A $\beta$  deposition adjusting for age in a large sample of both A $\beta$  positive and negative CN subjects and in AD patients.

We first determined the pattern of cortical thickness reductions and hippocampal volume loss in mild AD patients compared to CN subjects, and then investigated whether a similar pattern of A $\beta$ -associated volume loss was present in CN subjects. We also investigated the age-dependence of A $\beta$  deposition and of A $\beta$ -associated thickness reductions in both CN and AD, and quantified the extent and anatomic specificity of A $\beta$ -related volume loss within each group. We hypothesized that A $\beta$  deposition would be associated with local cortical thickness reductions in regions associated with the default network<sup>37</sup> at early stages of the pathophysiological process, prior to cognitive impairment.

## **Methods:**

*Subjects:* Participants were recruited from ongoing longitudinal studies in aging and during screening for dementia clinical trials at the Massachusetts General and Brigham and Women's Hospitals, and from several local referring tertiary memory clinics (Drs. Salloway, Marshall, and Marks). All participants were studied using protocols and informed consent procedures approved by the Partners Human Research Committee. All subjects underwent at least one comprehensive medical and psychiatric interview, as well as a neurological evaluation to rule out any major medical or neurological disorders that might contribute to cognitive dysfunction. None of the participants had any notable medical or neurological illness, and none had a history of alcoholism, drug abuse, or head trauma, or family history of autosomal dominant AD. None were clinically depressed (Geriatric Depression Scale <11) (Yesavage, 1982) or had other psychiatric illnesses. Each participant was scored on the Mini-Mental State Examination (MMSE)<sup>38</sup>, and also underwent a standard battery of neuropsychological (NP) tests, as reported previously<sup>23</sup>. The mean (sd) time between PET imaging and testing was 0.90 (1.9) months.

Subjects were classified into two groups, Clinically Normal (CN; N=87) and Alzheimer's disease (AD; N=32). All CN subjects had a Clinical Dementia Rating (CDR) score of 0<sup>39</sup>, MMSE > 27, and performance within 1.5 SD on age- and education adjusted norms on cognitive testing as detailed previously<sup>23</sup>. AD subjects were CDR=1 and satisfied criteria for a clinical diagnosis of probable AD according to National Institute of Neurological and Communication Disorders and Stroke / Alzheimer's disease and Related Disorders Association criteria<sup>40</sup>. Of the 87 CN subjects, 60 had APOE genotype data available: 47 were classified as  $\epsilon$ 4 negative (no 4-alleles) and 13 as  $\epsilon$ 4 positive (one or two 4-alleles).

*PET acquisition and processing:* 11C PiB PET was acquired and processed as described previously, using the distribution volume ratio (DVR) with cerebellar cortex as reference tissue<sup>18, 41</sup>. Detailed PET methods are in Supplemental Material.

MR acquisition and Freesurfer processing: High resolution MR imaging was acquired using MP-RAGE and processed with Freesurfer (FS) to measure cortical thickness and hippocampal volume, as described previously<sup>18, 19</sup>. The FS generated cortical parcellation defines a large precuneus region of interest (ROI) which overlaps areas of the posterior cingulate, including Brodmann area 23 and 31 along the posterior midline<sup>42</sup>; we therefore denoted this cortical ROI as the PCC (posterior cingulate/precuneus) in the following. Further details of FS processing are in Supplemental Material.

Choice of proxy region for A $\beta$  deposition: As proxy ROI for A $\beta$  deposition, we chose the PCC because it is a highly vulnerable, common site of early involvement. In addition, however, we evaluated nine other ROIs that are also vulnerable to A $\beta$  deposition to determine whether A $\beta$ -associated volume/thickness changes differed when the proxy measure of PiB retention was from these alternative ROIs: rostral anterior cingulate, medial orbitofrontal, rostral middle frontal, caudal anterior cingulate, precuneus, superior frontal, pars opercularis, caudal middle frontal, inferior parietal, lateral orbitofrontal, and global.

Dichotomization of PiB data: Like earlier studies<sup>2, 18, 19, 23, 34</sup>, we chose a threshold of amyloid positivity that is somewhat arbitrary, since a rigorous definition will likely require longitudinal followup. As in a previous report<sup>18</sup> we split the CN group based on partial volume corrected (PVC) PCC PiB retention: subject with PCC DVR>1.60 were classified as “CN+“ (PiB-positive CN), and those with DVR<=1.60 as “CN-“. This is a conservative threshold and classifies fewer CN as PiB+ relative to other criteria (e.g., Hedden et al.<sup>19</sup>). As described below, all analyses were also performed without the use of a threshold.

Statistical Analyses: We evaluated the relation of hippocampal volume and cortical thickness to PiB primarily by treating PiB DVR as a continuous variable. Regression models were used to examine the relationship of hippocampal volume and cortical thickness to A $\beta$  burden in CN and AD groups; regression

coefficients for all models were estimated by ordinary least squares. At each cortical vertex thickness was taken as the dependent variable, and PVC PCC PiB DVR and age were taken as independent variables. Clusters of vertices with thickness-DVR regression coefficient p-values exceeding a predetermined threshold ( $p=0.05$ ) were identified, and cluster-wise statistical significances were calculated via 5000 instances of a Monte Carlo simulation, based on the noise distribution of the baseline analysis<sup>43</sup>. We evaluated the relationship of hippocampal volume to PiB retention using similar regression models, with gender added as a covariate (see below)<sup>11, 44-46</sup>. Hippocampal volumes (sum of volumes in left and right hemisphere) were covariance adjusted for total intracranial volume as measured by estimated total intracranial volume (eTIV) over the full sample prior to inclusion in the regression equation as the dependent variable<sup>47</sup>.

Parallel analyses were performed with regional average cortical thicknesses (average of left and right hemisphere thicknesses) from a set of anatomically defined cortical ROI: global (average over all cortical ROI), inferior parietal, PCC, parahippocampal and entorhinal<sup>26</sup>. ROI thickness was taken as the dependent variable, and PiB DVR and age as independent variables.

A hypothetical model of the relationship of cortical thickness and PiB retention was assessed under the assumption that both followed sigmoidal curves, parameterized by a common time-like parameter (Supplemental Materials).

The age dependence of cortical thickness or hippocampal volume was investigated by regressing thickness on age, or volume on age and gender, in both the CN and AD diagnostic groups. Volume or thickness contrasts between diagnostic groups (CN and AD, or CN- and CN+) were assessed by ANCOVA implemented as a general linear model, with age and gender covariates for volume, or age covariate for thickness.

Differences in eTIV-adjusted hippocampal volume between diagnostic groups were assessed by ANCOVA implemented as a general linear model, with age and gender covariates; similar models excluding the gender covariate were used to assess cortical thickness differences between the same groups.

In order to test whether age differences of cortical thickness or PiB uptake depended on APOE carrier status in the CN group,  $\epsilon 4$  status (positive if one or two 4-alleles, negative otherwise) was added as a factor to the model and allowed to interact with the regression term. Similarly, the differential effect of APOE status on the relationship of cortical thickness and PiB uptake in the CN group was assessed by including carrier status as a factor interacting with the thickness-PiB regression term.

The capacity of regional cortical average thickness to discriminate between the CN- and CN+ groups was assessed by logistic regression followed by ROC curve analysis. Group membership probabilities predicted by the logistic regression model with thickness and age regressors were used to construct a ROC curve, and the area under the curve (AUC) and its statistical significance were computed (Wilcoxon rank sum test with continuity correction).

## **Results:**

### **Subject characteristics**

AD and CN groups differed in MMSE scores and PCC PiB retention, but not in age, gender, or education (Table 1). Hippocampal volumes were slightly greater in men compared to women even after residualization by intracranial volume (data not shown). Gender was therefore included as a factor in regression models involving hippocampal volume. Gender effects were not detected in PiB or cortical thickness data.

### **Thickness/volume contrasts in AD versus CN**

Reduced temporoparietal cortical thickness, controlling for age, was seen in AD compared to CN (Supplemental Figure S1). Thickness decreases in AD relative to CN ranged up to 0.20 mm (first/second/third quartiles = 0.10/0.13/0.15 mm for vertices in the PCC). The anatomic pattern included posterior cingulate extending into the precuneus, inferior and superior parietal lobules, superior, middle and inferior temporal, fusiform, entorhinal, parahippocampal, perirolandic, and posterior prefrontal regions. Anterior and medial prefrontal regions were less involved (Supplemental Figure S1). In ROI contrasts, AD subjects had lower hippocampal volume ( $p < 10^{-5}$ ) and decreased entorhinal, parahippocampal, PCC, inferior parietal, and global thickness ( $p < 10^{-5}$ ), compared to the CN group (Supplemental Figure S2).

### **A $\beta$ -associated cortical thickness/volume reductions in AD and CN**

*Continuous A $\beta$  (vertex-level analyses):* Treating PCC PiB retention as a continuous measure and controlling for age, A $\beta$ -associated cortical thickness reductions in both AD and CN subjects were seen in posterior cingulate extending into the precuneus, inferior parietal lobule, superior parietal, lateral temporal

and lateral prefrontal (Figure 1). In contrast to the AD vs. CN thickness contrast maps in Supplemental Figure S1, medial temporal cortical A $\beta$ -associated thickness reductions were not observed. No regions exhibited significant cortical thickness increases with increasing PiB retention.

In the CN group, cluster-wise statistical significance of vertex-level regression coefficients was assessed by Monte Carlo simulation to correct for capitalization on multiple comparisons. We identified seven clusters of vertices as exhibiting significant thickness reductions with increasing A $\beta$  at  $p < 0.05$  (corrected): right posterior cingulate/precuneus, left inferior parietal, left and right rostral middle frontal, left and right supramarginal, and right superior temporal (Table 2 and Supplemental Figure S3). There were no areas of significant interaction between APOE carrier status and age-adjusted A $\beta$ -associated thickness variation in the CN group (N=60; data not shown), indicating that thickness-PiB regression slopes did not differ according to carrier status. To confirm that the observed significant inverse relation of A $\beta$  and thickness was not an artifact of the PET partial volume correction, we substituted non-PVC PiB DVR for PVC DVR in the vertex-based regressions. Statistical significance of coefficients in the non-PVC analyses were lower in the CN group, as expected due to contraction of PET DVR ranges, but the pattern of the effects did not change (Supplemental Figure S4).

*Continuous A $\beta$  (ROI-level analyses):* Data in ROI were expressed as age-adjusted structural change per unit change in PiB retention for hippocampal volume (mm<sup>3</sup>/DVR) and cortical thickness (mm/DVR) (Figure 2). Significant A $\beta$ -associated cortical thickness reduction (significant negative regression coefficient expressing change in thickness per unit increase in DVR) was confirmed in PCC, inferior parietal, and global ROI, but entorhinal and parahippocampal thickness and hippocampal volume variations with A $\beta$  were not statistically significant.

*CN Group dichotomized into CN-/CN+ by A $\beta$  level:* The vertex-level contrast of CN- vs. CN+ groups revealed age-adjusted thickness reduction in the CN+ group prominently in posterior

cingulate/precuneus, lateral parietal, and prefrontal cortices (Supplemental Figure S5). Thickness decreases in CN+ relative to CN- ranged up to 0.095 mm (first/second/third quartiles = 0.017/0.032/0.045 mm for vertices in the PCC). In ROI contrasts of CN- vs. CN+ groups, lower ROI average thicknesses were observed in the CN+ group but the differences did not reach statistical significance possibly because of lower sensitivity (Supplemental Figure S2). Using PCC thickness to discriminate CN- and CN+ subjects yielded a statistically significant ( $p < 0.05$ ) logistic regression model in which a 0.1 mm decrease was associated with an odds-ratio of 1.60. The corresponding AUC=0.70 ( $p < 0.01$ ), holding age constant at its grand mean. Other regions examined (parietal, frontal, or global average) did not achieve a similar discriminative efficiency.

### **Thickness- $A\beta$ sigmoid modeling**

While  $A\beta$ -associated thinning was observed in CN subjects as described above, 1) thinning was more anatomically extensive in the AD group; and 2) significantly more thinning per unit DVR was observed in the AD group (e.g., 0.4 mm/DVR in medial and lateral parietal areas) than in the CN group (Figure 1). A vertex-level assessment of the difference revealed a significant interaction of the thickness-versus- $A\beta$  coefficient and clinical status factor (CN versus AD) in posterior midline and inferior parietal regions ( $p < 10^{-4}$ ; data not shown). We related these observations to candidate time courses along the hypothetical CN-AD trajectory (See Supplemental Material), in which the data were evaluated using sigmoid models to relate PCC cortical thickness and PiB retention. Assuming sigmoid time functions for PiB increase and loss of cortical thickness, both with the same rate-of-change achieved at the midpoint of the S-shaped portion of the curves, we calculated how far apart in time these midpoints would have to be in order to achieve the best fit to our data. In fitting this model to the age-adjusted CN and AD group data (Figure 3;  $r\text{-sq} = 0.48$ ;  $p < 10^{-4}$ ) we calculated this time lag parameter (see Supplemental Material) to be

equal to 0.35 times the amyloid saturation time (the time to go from zero to maximum amyloid). For example, if a 10-year amyloid saturation time were hypothesized, the time lag between the rapid phases of PiB increase and cortical thinning would be 3.5 years.

### **Age dependence of thickness/volume and of PiB retention in CN and AD**

Vertex-level analyses revealed that greater age was associated with reduced thickness among CN subjects in perirolandic, lateral and inferior temporal, superior parietal, posterior cingulate and precuneus cortices ( $p < 0.0001$ , uncorrected for multiple comparisons; see Supplemental Figure S6). The vertex-based findings were confirmed in cortical ROI, where age-related reductions were also seen in parahippocampal, inferior parietal and global cortical thickness, and marginally in entorhinal thickness in the CN group. Age associated hippocampal volume reduction was also significant in the CN group. In the AD group, greater age was associated with decreased volume in hippocampus and reduced thickness prominently in parahippocampal cortex (Supplemental Figure S6).

Analyses of PiB data derived either from vertices or from confirmatory ROI revealed that while higher PiB retention in precuneus/posterior cingulate, anterior cingulate, and prefrontal regions was associated with greater age in the CN group, the inverse relation was seen in the AD group (Supplemental Figure S7). For example, age was associated with increased PCC ROI PiB retention in the CN group ( $p < 0.001$ ), but with decreased PCC retention in the AD group ( $p < 0.005$ ). This corresponded to a significant difference in the regression line slopes between the two groups ( $p < 10^{-4}$ ). Prominently reduced A $\beta$  deposition as a function of age was observed in medial occipital regions in AD (Supplemental Figure S7). When non-PVC data were used, the age associations were similar but less robust possibly due to the narrower ranges of uncorrected DVR (data not shown).

There were no areas of significant interaction between APOE carrier status and variation with age of cortical thickness or PiB retention in the CN group (N=60; data not shown).

### **Differential impact of age and A $\beta$ deposition on hippocampal volume and cortical thickness**

Maps of cortical thickness for the age regression coefficient were computed with the A $\beta$  deposition term also included in the model. These were nearly identical to the maps of the simple age-dependence (Supplemental Figure S6), indicating that the age was inversely related to thickness independent of A $\beta$  deposition (data not shown).

Using ROI data we evaluated a regression model that included age, gender and PCC PiB retention as predictors of PCC ROI thickness or hippocampal ROI volume. PCC thickness was independently associated with both age ( $p < 10^{-3}$ ) and A $\beta$  deposition ( $p < 0.004$ ). In contrast, hippocampal volume was associated with age ( $p < 10^{-5}$ ) but not with A $\beta$  deposition ( $p = 0.38$ ). Gender was not related to either hippocampal volume (pre-adjusted for eTIV;  $p < 0.07$ ) or PCC thickness ( $p < 0.45$ ). When added to the models, the age-by-A $\beta$  interaction term was not significant in either case. Thus, covarying A $\beta$  deposition, greater age was associated with reduced hippocampal volume and PCC thickness; however, covarying age, A $\beta$  deposition was associated with reduced PCC thickness but not with reduced hippocampal volume.

### **Choice of proxy for PiB retention**

We tested the hypothesis that results using alternative, non-PCC regions would differ from those in which the PCC was used as the proxy for A $\beta$  deposition. We found that using as proxy the rostral anterior cingulate, rostral middle frontal, or inferior parietal cortices all yielded similar patterns of A $\beta$ -associated cortical thinning, which was not surprising given the high correlation of PiB retention in these

regions with PiB retention in the PCC (Pearson correlations ranged from 0.80 to 0.89) In contrast, hippocampus PiB retention was not significantly related to thinning in any cortical region (data not shown).

## **Discussion:**

The major finding of this study is that significant A $\beta$ -associated cortical thinning occurs among clinically normal older individuals in a pattern consistent with early AD. While this finding supports the possibility that A $\beta$  deposition in normal individuals represents preclinical AD, direct observation with longitudinal data will be required to evaluate the strength and timing of this link. Our data suggest that A $\beta$ -associated neurodegeneration manifests as cortical thinning in regions vulnerable to early A $\beta$  deposition, including association cortices along the posterior medial wall and lateral parietal cortex. In particular, we observed thinning in the inferior parietal lobule and the posterior cingulate extending into the precuneus, which are regions that form nodes of a large-scale cortical system known as the default network<sup>37,48, 49</sup>. This system has been implicated in both memory-related function and in amyloid- and AD-related memory dysfunction<sup>18, 37, 49-52</sup>. Our findings are consistent with a pathophysiologic link between A $\beta$  deposition and neurodegeneration in this network, which may anticipate memory failure and progression to clinical dementia<sup>18, 19, 21, 37, 53</sup>.

Along the posterior midline, the posterior cingulate and retrosplenial cortex are anatomically connected to medial temporal structures, and we found that while the hippocampus and MTL cortices demonstrated significant age-associated atrophy, the association of MTL atrophy with A $\beta$  deposition was variable in these asymptomatic older individuals. While our results are consistent with the hypothesis that MTL atrophy coincides with the emergence of manifest cognitive impairment<sup>2, 54, 55</sup>, we did not observe a

significant difference between MTL and cortical atrophy, and thus cannot order the relative timing of effects with the present data. While macroscopically visible cortical atrophy is associated with dementia, it is not generally observed in non-demented individuals at postmortem<sup>56</sup>, perhaps because of an inability to differentiate it from normal age-associated atrophy. Our data suggest that the A $\beta$  deposition commonly detected in normal older individuals is associated with subtle posterior cingulate and parietal neurodegeneration that occurs prior to, and may be a harbinger of, clinically significant impairment<sup>29</sup>. It is possible that further investigation will reveal evidence of subtle cognitive alterations related to cortical thinning even within clinically normal individuals, particularly when the level of cognitive reserve is considered<sup>23</sup>.

More broadly, our findings should be considered in the context of a putative sequence of events in AD pathology that can be observed with biomarkers. Using a largely biphasic model of disease sequence, A $\beta$  deposition has been hypothesized to occur early in the sequence of AD pathology and to be followed later by neurodegeneration, which is then related to the symptomatic phases of the disease, cognitive decline and dementia<sup>57-59</sup>. Our present findings and those of earlier studies<sup>29,33,34</sup> that suggest PiB retention is correlated with cortical thinning in normal individuals raise the possibility that the hypothesized lag period between A $\beta$  deposition and neurodegeneration may be shorter than previously thought. A precise mechanism by which A $\beta$  deposition could be linked to neurodegeneration has not been firmly established. It is possible that toxic effects of A $\beta$  oligomeric assemblies that surround fibrillar forms could be exerted locally early in the process and result directly in synapse and cell loss<sup>60, 61</sup>. Such a mechanism entails a direct relationship between the presence of A $\beta$  and neurodegeneration, which could potentially be observed with sensitive biomarkers. However, while the sensitivity of A $\beta$  imaging may be improved in the future and permit better detection, individuals with predominantly pre-fibrillar or

polymorphic forms of A $\beta$  that are refractory to PiB would not be detectable with PiB or likely with other thioflavin or Congo-red derivatives<sup>62-64</sup>.

We found that A $\beta$  and PCC thickness were more strongly correlated in AD than in CN (see Figure 1) and evaluated these data according to a recently proposed model<sup>58</sup> in which A $\beta$  deposition and cortical thickness follow sigmoid-shaped curves in time. We simultaneously fit sigmoid models to PCC PiB and age-adjusted thickness data for the combined CN and AD groups, and determined the temporal lag between the dynamic phases of amyloid accumulation and cortical thinning to be approximately 35% of the total time required for amyloid to rise from its baseline to maximum. It should be emphasized that the model in its particularities as presented here is tentative, and should be considered as a schematic rather than definitive treatment of the problem. Such modeling will remain speculative as to accurate parameters of the underlying sigmoid curves until longitudinal data are available.

While AD neurodegeneration is well established to occur prominently in the MTL<sup>54, 55, 65</sup> and to be correlated with neurofibrillary pathology<sup>66</sup>, our findings are consistent with emerging evidence that thinning in posterior association cortices is also a prominent feature of MCI and AD<sup>11, 29, 37, 67</sup>. While the measured amount of age-adjusted thickness reduction per unit of PiB retention (DVR) was approximately the same in posterior cingulate/precuneus and in MTL structures, the standard errors were larger in the MTL (see Figure 1) and the regression coefficients did not reach significance. Future work with a larger data sample will be required to order the relative emergence of effects between posterior cingulate and MTL structures. Neurofibrillary tangle pathology may partially explain this observation of greater variability in the MTL, since it is common in MTL but rarely widespread in cortex of CN subjects<sup>56, 57, 66, 68</sup>. Our data are not consistent with previous observations that A $\beta$  deposition is only seen after significant neurofibrillary tangle deposition and MTL atrophy<sup>68</sup>, but instead suggest that the pathologic sequence of events in preclinical AD is one in which A $\beta$  deposition is related to neurodegeneration in posterior

cingulate and distributed regions of association neocortex that occurs along with or possibly even prior to hippocampal and entorhinal neurodegeneration.

Previous reports of the relation of PiB retention and hippocampal volume in CN subjects have been inconsistent. Some reported an inverse relation (i.e. decreased volume with increased PiB retention) in CN subjects<sup>33,34</sup>, while others found such a relation only among the A $\beta$ -positive CN group<sup>35</sup> or only in CN subjects with subjective cognitive impairment<sup>69</sup>. These studies have differed in their treatment of the potentially confounding effect of age on both A $\beta$  level and atrophy. We evaluated hippocampal volume, cortical thickness, and PiB retention for evidence of age dependence and found evidence for an age effect in all domains. The age dependence of volume/thickness across a broad age range has been previously reported<sup>70</sup>, and although some investigators have not found a significant impact of age within a more restricted older age range<sup>29</sup>, others have applied an age-adjustment to thickness/volume data<sup>11</sup>. The strong age dependence of A $\beta$  deposition we observed in CN subjects is consistent with neuropathological studies that inferred from cross-sectional data that A $\beta$  gradually accumulates with age<sup>68</sup>. Several previous PiB studies<sup>9, 16, 71</sup> did not report evidence of a significant relationship with age, perhaps due to the small sample sizes with limited age ranges, although a recent study did demonstrate an age association<sup>72</sup>. Morris et al. found that the age dependence of PiB data was largely accounted for by the strong age association with PiB retention among carriers of the APOE4 allele<sup>34, 73</sup>, likely a reflection of the sample enrichment for younger CN subjects with positive family histories. We did not find an interaction of the age-A $\beta$  relationship with APOEe4 carrier status among the subset of subjects on whom genotypes were available (data not shown).

Interestingly, the age dependence of A $\beta$  deposition among CN subjects was reversed in AD patients, such that greater age was associated with lower levels of A $\beta$  deposition. The reversal of the A $\beta$ -age coefficient in the AD group compared to the CN group could be due to a survivor effect, such that

older subjects with greater amounts of A $\beta$  were too impaired (e.g., MMSE < 18) to have been included in our study. Other potential factors, including an age-related change in PiB binding sites or affinity or a change in the production or clearance of A $\beta$ <sup>74, 75</sup>, will require further study. Moreover, longitudinal observation over long intervals may be required to determine whether individual AD patients' levels of A $\beta$  decline over time, which has not been observed in longitudinal PiB data that has spanned 1-2 years<sup>2, 5, 76</sup>.

In summary, our findings provide support for the hypothesis that A $\beta$  is associated with local neurodegeneration in key nodes of a distributed network supporting memory processes, and that this process begins prior to clinically evident cognitive impairment, but continues into the stage of clinical dementia. Longitudinal follow-up of these clinically normal older individuals is ongoing to determine if the combination of A $\beta$  burden and volumetric loss is predictive of incipient cognitive decline, and progression to AD dementia.

#### Acknowledgements:

This work was supported by the National Institute on Aging (R01-AG027435-S1, R.A.S., K.A.J.; P50-AG00513421, K.A.J., R.A.S.; P01-AG036694, R.A.S., K.A.J, R.L.B; and R01-AG021910, R.L.B.), an anonymous medical foundation, the Howard Hughes Medical Institute (R.L.B.), the Alzheimer Association (grant IIRG-06-32444, R.A.S., K.A.J. and grant IIRG-08-90934, D.M.R., K.A.J.), the Charles H. Farnsworth Trust, Boston Massachusetts (D.M.R.).

We thank the investigators and staff of the Massachusetts Alzheimer's Disease Research Center, the individual research participants, and their families and caregivers.

#### References:

1. Price JL, Morris JC. Tangles and plaques in nondemented aging and "preclinical" Alzheimer's disease. *Ann Neurol*. 1999;45:358-368
2. Jack CR, Jr., Lowe VJ, Weigand SD et al. Serial PIB and MRI in normal, mild cognitive impairment and Alzheimer's disease: implications for sequence of pathological events in Alzheimer's disease. *Brain*. 2009;132:1355-1365
3. Ingelsson M, Fukumoto H, Newell KL et al. Early A $\beta$  accumulation and progressive synaptic loss, gliosis, and tangle formation in AD brain. *Neurology*. 2004;62:925-931
4. Mintun MA, Larossa GN, Sheline YI et al. [ $^{11}\text{C}$ ]PIB in a nondemented population: potential antecedent marker of Alzheimer disease. *Neurology*. 2006;67:446-452
5. Engler H, Forsberg A, Almkvist O et al. Two-year follow-up of amyloid deposition in patients with Alzheimer's disease. *Brain*. 2006;129:2856-2866

6. Jack CR, Jr., Lowe VJ, Senjem ML et al. 11C PiB and structural MRI provide complementary information in imaging of Alzheimer's disease and amnesic mild cognitive impairment. *Brain*. 2008;131:665-680
7. Hyman BT, Flory JE, Arnold SE et al. Quantitative assessment of ALZ-50 immunoreactivity in Alzheimer's disease. *J Geriatr Psychiatry Neurol*. 1991;4:231-235
8. Arnold SE, Hyman BT, Flory J et al. The topographical and neuroanatomical distribution of neurofibrillary tangles and neuritic plaques in the cerebral cortex of patients with Alzheimer's disease. *Cereb Cortex*. 1991;1:103-116
9. Klunk WE, Engler H, Nordberg A et al. Imaging brain amyloid in Alzheimer's disease with Pittsburgh Compound-B. *Ann Neurol*. 2004;55:306-319
10. Jack CR, Jr., Petersen RC, Xu YC et al. Medial temporal atrophy on MRI in normal aging and very mild Alzheimer's disease. *Neurology*. 1997;49:786-794
11. Desikan RS, Cabral HJ, Hess CP et al. Automated MRI measures identify individuals with mild cognitive impairment and Alzheimer's disease. *Brain*. 2009;132:2048-2057
12. Fischl B, van der Kouwe A, Destrieux C et al. Automatically parcellating the human cerebral cortex. *Cereb Cortex*. 2004;14:11-22
13. Katzman R, Terry R, DeTeresa R et al. Clinical, pathological, and neurochemical changes in dementia: a subgroup with preserved mental status and numerous neocortical plaques. *Ann Neurol*. 1988;23:138-144
14. Arriagada PV, Marzloff K, Hyman BT. Distribution of Alzheimer-type pathologic changes in nondemented elderly individuals matches the pattern in Alzheimer's disease. *Neurology*. 1992;42:1681-1688

15. Bennett DA, Schneider JA, Wilson RS et al. Education modifies the association of amyloid but not tangles with cognitive function. *Neurology*. 2005;65:953-955
16. Aizenstein HJ, Nebes RD, Saxton JA et al. Frequent amyloid deposition without significant cognitive impairment among the elderly. *Arch Neurol*. 2008;65:1509-1517
17. Gomperts SN, Rentz DM, Moran E et al. Imaging amyloid deposition in Lewy body diseases. *Neurology*. 2008;71:903-910
18. Sperling RA, Laviolette PS, O'Keefe K et al. Amyloid deposition is associated with impaired default network function in older persons without dementia. *Neuron*. 2009;63:178-188
19. Hedden T, Van Dijk KR, Becker JA et al. Disruption of functional connectivity in clinically normal older adults harboring amyloid burden. *J Neurosci*. 2009;29:12686-12694
20. Morris JC, Roe CM, Grant EA et al. Pittsburgh compound B imaging and prediction of progression from cognitive normality to symptomatic Alzheimer disease. *Arch Neurol*. 2009;66:1469-1475
21. Sheline YI, Raichle ME, Snyder AZ et al. Amyloid plaques disrupt resting state default mode network connectivity in cognitively normal elderly. *Biol Psychiatry*. 2010;67:584-587
22. Pike KE, Savage G, Villemagne VL et al. Beta-amyloid imaging and memory in non-demented individuals: evidence for preclinical Alzheimer's disease. *Brain*. 2007;130:2837-2844
23. Rentz DM, Locascio JJ, Becker JA et al. Cognition, Reserve, and Amyloid Deposition in Normal Aging. *Ann Neurol*. 2010;67:353-364
24. Fischl B, Dale AM. Measuring the thickness of the human cerebral cortex from magnetic resonance images. *Proc Natl Acad Sci U S A*. 2000;97:11050-11055
25. Lerch JP, Pruessner JC, Zijdenbos A et al. Focal decline of cortical thickness in Alzheimer's disease identified by computational neuroanatomy. *Cereb Cortex*. 2005;15:995-1001

26. Desikan RS, Segonne F, Fischl B et al. An automated labeling system for subdividing the human cerebral cortex on MRI scans into gyral based regions of interest. *Neuroimage*. 2006;31:968-980
27. Vemuri P, Gunter JL, Senjem ML et al. Alzheimer's disease diagnosis in individual subjects using structural MR images: validation studies. *Neuroimage*. 2008;39:1186-1197
28. Scahill RI, Schott JM, Stevens JM et al. Mapping the evolution of regional atrophy in Alzheimer's disease: unbiased analysis of fluid-registered serial MRI. *Proc Natl Acad Sci U S A*. 2002;99:4703-4707
29. Dickerson BC, Bakkour A, Salat DH et al. The cortical signature of Alzheimer's disease: regionally specific cortical thinning relates to symptom severity in very mild to mild AD dementia and is detectable in asymptomatic amyloid-positive individuals. *Cereb Cortex*. 2009;19:497-510
30. Bakkour A, Morris JC, Dickerson BC. The cortical signature of prodromal AD: regional thinning predicts mild AD dementia. *Neurology*. 2009;72:1048-1055
31. Du AT, Schuff N, Kramer JH et al. Different regional patterns of cortical thinning in Alzheimer's disease and frontotemporal dementia. *Brain*. 2007;130:1159-1166
32. Davatzikos C, Xu F, An Y et al. Longitudinal progression of Alzheimer's-like patterns of atrophy in normal older adults: the SPARE-AD index. *Brain*. 2009;132:2026-2035
33. Mormino EC, Kluth JT, Madison CM et al. Episodic memory loss is related to hippocampal-mediated beta-amyloid deposition in elderly subjects. *Brain*. 2009;132:1310-1323
34. Storandt M, Mintun MA, Head D, Morris JC. Cognitive decline and brain volume loss as signatures of cerebral amyloid-beta peptide deposition identified with Pittsburgh compound B: cognitive decline associated with A $\beta$  deposition. *Arch Neurol*. 2009;66:1476-1481
35. Bourgeat P, Chetelat G, Villemagne VL et al. Beta-amyloid burden in the temporal neocortex is related to hippocampal atrophy in elderly subjects without dementia. *Neurology*. 2010;74:121-127

36. Chetelat G, Villemagne VL, Bourgeat P et al. Relationship between atrophy and beta-amyloid deposition in Alzheimer's disease. *Ann Neurol.* 2010;67:317-324
37. Buckner RL, Snyder AZ, Shannon BJ et al. Molecular, structural, and functional characterization of Alzheimer's disease: evidence for a relationship between default activity, amyloid, and memory. *J Neurosci.* 2005;25:7709-7717
38. Folstein MF, Folstein SE, McHugh PR. "Mini-mental state". A practical method for grading the cognitive state of patients for the clinician. *J Psychiatr Res.* 1975;12:189-198
39. Morris JC. The Clinical Dementia Rating (CDR): current version and scoring rules. *Neurology.* 1993;43:2412-2414
40. McKhann G, Drachman D, Folstein M et al. Clinical diagnosis of Alzheimer's disease: report of the NINCDS-ADRDA Work Group under the auspices of Department of Health and Human Services Task Force on Alzheimer's Disease. *Neurology.* 1984;34:939-944
41. Johnson KA, Gregas M, Becker JA et al. Imaging of amyloid burden and distribution in cerebral amyloid angiopathy. *Ann Neurol.* 2007;62:229-234
42. Vogt BA, Vogt L, Laureys S. Cytology and functionally correlated circuits of human posterior cingulate areas. *Neuroimage.* 2006;29:452-466
43. Hayasaka S, Nichols TE. Validating cluster size inference: random field and permutation methods. *Neuroimage.* 2003;20:2343-2356
44. Jack CR, Jr., Petersen RC, O'Brien PC, Tangalos EG. MR-based hippocampal volumetry in the diagnosis of Alzheimer's disease. *Neurology.* 1992;42:183-188
45. Whitwell JL, Shiung MM, Przybelski SA et al. MRI patterns of atrophy associated with progression to AD in amnesic mild cognitive impairment. *Neurology.* 2008;70:512-520

46. Frisoni GB, Fox NC, Jack CR, Jr. et al. The clinical use of structural MRI in Alzheimer disease. *Nat Rev Neurol.* 2010;6:67-77
47. Buckner RL, Head D, Parker J et al. A unified approach for morphometric and functional data analysis in young, old, and demented adults using automated atlas-based head size normalization: reliability and validation against manual measurement of total intracranial volume. *Neuroimage.* 2004;23:724-738
48. Gusnard DA, Akbudak E, Shulman GL, Raichle ME. Medial prefrontal cortex and self-referential mental activity: relation to a default mode of brain function. *Proc Natl Acad Sci U S A.* 2001;98:4259-4264
49. Buckner RL, Sepulcre J, Talukdar T et al. Cortical hubs revealed by intrinsic functional connectivity: mapping, assessment of stability, and relation to Alzheimer's disease. *J Neurosci.* 2009;29:1860-1873
50. Lustig C, Snyder AZ, Bhakta M et al. Functional deactivations: change with age and dementia of the Alzheimer type. *Proc Natl Acad Sci U S A.* 2003;100:14504-14509
51. Daselaar SM, Prince SE, Cabeza R. When less means more: deactivations during encoding that predict subsequent memory. *Neuroimage.* 2004;23:921-927
52. Wagner AD, Shannon BJ, Kahn I, Buckner RL. Parietal lobe contributions to episodic memory retrieval. *Trends Cogn Sci.* 2005;9:445-453
53. Andrews-Hanna JR, Snyder AZ, Vincent JL et al. Disruption of large-scale brain systems in advanced aging. *Neuron.* 2007;56:924-935
54. Fox NC, Warrington EK, Rossor MN. Serial magnetic resonance imaging of cerebral atrophy in preclinical Alzheimer's disease. *Lancet.* 1999;353:2125

55. Kaye JA, Swihart T, Howieson D et al. Volume loss of the hippocampus and temporal lobe in healthy elderly persons destined to develop dementia. *Neurology*. 1997;48:1297-1304
56. Savva GM, Wharton SB, Ince PG et al. Age, neuropathology, and dementia. *N Engl J Med*. 2009;360:2302-2309
57. Bennett DA, Schneider JA, Wilson RS et al. Neurofibrillary tangles mediate the association of amyloid load with clinical Alzheimer disease and level of cognitive function. *Arch Neurol*. 2004;61:378-384
58. Jack CR, Jr., Knopman DS, Jagust WJ et al. Hypothetical model of dynamic biomarkers of the Alzheimer's pathological cascade. *Lancet Neurol*;9:119-128
59. Gomez-Isla T, Price JL, McKeel DW, Jr. et al. Profound loss of layer II entorhinal cortex neurons occurs in very mild Alzheimer's disease. *J Neurosci*. 1996;16:4491-4500
60. Walsh DM, Selkoe DJ. A beta oligomers - a decade of discovery. *J Neurochem*. 2007;101:1172-1184
61. Shankar GM, Li S, Mehta TH et al. Amyloid-beta protein dimers isolated directly from Alzheimer's brains impair synaptic plasticity and memory. *Nat Med*. 2008;14:837-842
62. Lockhart A, Lamb JR, Osredkar T et al. PIB is a non-specific imaging marker of amyloid-beta (A $\beta$ ) peptide-related cerebral amyloidosis. *Brain*. 2007;130:2607-2615
63. Rosen RF, Ciliax BJ, Wingo TS et al. Deficient high-affinity binding of Pittsburgh compound B in a case of Alzheimer's disease. *Acta Neuropathol*. 2010;119:221-233
64. Leinonen V, Alafuzoff I, Aalto S et al. Assessment of beta-amyloid in a frontal cortical brain biopsy specimen and by positron emission tomography with carbon 11-labeled Pittsburgh Compound B. *Arch Neurol*. 2008;65:1304-1309

65. Jack CR, Jr., Petersen RC, Xu Y et al. Rate of medial temporal lobe atrophy in typical aging and Alzheimer's disease. *Neurology*. 1998;51:993-999
66. Vemuri P, Whitwell JL, Kantarci K et al. Antemortem MRI based SStructural Abnormality iNDex (STAND)-scores correlate with postmortem Braak neurofibrillary tangle stage. *Neuroimage*. 2008;42:559-567
67. Fjell AM, Walhovd KB, Fennema-Notestine C et al. Brain atrophy in healthy aging is related to CSF Levels of A $\beta$ 1-42. *Cereb Cortex*. 2010;20:2069-2079
68. Braak H, Braak E. Frequency of stages of Alzheimer-related lesions in different age categories. *Neurobiol Aging*. 1997;18:351-357
69. Chetelat G, Villemagne VL, Bourgeat P et al. Relationship between atrophy and beta-amyloid deposition in Alzheimer disease. *Ann Neurol*;67:317-324
70. Salat DH, Buckner RL, Snyder AZ et al. Thinning of the cerebral cortex in aging. *Cereb Cortex*. 2004;14:721-730
71. Rowe CC, Ng S, Ackermann U et al. Imaging beta-amyloid burden in aging and dementia. *Neurology*. 2007;68:1718-1725
72. Resnick SM, Sojkova J, Zhou Y et al. Longitudinal cognitive decline is associated with fibrillar amyloid-beta measured by [11C]PiB. *Neurology*;74:807-815
73. Morris JC, Roe CM, Xiong C et al. APOE predicts amyloid-beta but not tau Alzheimer pathology in cognitively normal aging. *Ann Neurol*. 2010;67:122-131
74. Hyman BT. The neuropathological diagnosis of Alzheimer's disease: clinical-pathological studies. *Neurobiol Aging*. 1997;18:S27-32
75. Wegiel J, Wisniewski HM, Morys J et al. Neuronal loss and beta-amyloid removal in the amygdala of people with Down syndrome. *Neurobiol Aging*. 1999;20:259-269

76. Rinne JO, Brooks DJ, Rossor MN et al. 11C-PiB PET assessment of change in fibrillar amyloid-beta load in patients with Alzheimer's disease treated with bapineuzumab: a phase 2, double-blind, placebo-controlled, ascending-dose study. *Lancet Neurol*;9:363-372

**Table 1:****Table 1: Demographics**

	CN All**	CN-	CN+	AD	All
CDR	0	0	0	1	0 or 1
N (%F)	86 (66)	68 (65)	18 (67)	32 (44)	118 (60)
Age, yr	*75 ± 8 (55 - 90)	73 ± 8 (55 - 89)	79 ± 5 (69 - 90)	72 ± 9 (57 - 84)	74 ± 8 (55 - 90)
MMSE	29 ± 1 (27 - 30)	29 ± 1 (27 - 30)	29 ± 1 (27 - 30)	22 ± 4 (18 - 27)	27 ± 4 (18 - 30)
Education, yr	16 ± 3 (12 - 24)	16 ± 3 (12 - 24)	16 ± 3 (12 - 20)	18 ± 1 (16 - 20)	16 ± 3 (12 - 24)
PCC DVR	1.39 ± 0.31 (0.98 - 2.40)	1.25 ± 0.13 (0.98 - 1.58)	<sup>γ</sup> 1.91 ± 0.25 (1.61 - 2.40)	<sup>δ</sup> 2.35 ± 0.39 (1.36 - 2.97)	1.65 ± 0.54 (0.98 - 2.97)

\* Mean ± SD (range)

\*\* Abbreviations: CN, cognitively normal; AD, Alzheimer's disease; PCC, Posterior cingulate/precuneus;

DVR, distribution volume ratio; CDR, Clinical Dementia Rating;

CN- or CN+, CN subjects with PCC PiB DVR ≤ or >1.60

F, female; MMSE, Mini-Mental State Examination

<sup>α</sup> Differs from CN- (p<0.002)

<sup>β</sup> Differs from CN- and CN+ (p<10<sup>-5</sup>)

<sup>γ</sup> Differs from CN- (p<10<sup>-5</sup>)

<sup>δ</sup> Differs from CN- and CN+ (p<10<sup>-5</sup>)

**Table 2:**

**Table 2: Reduction of vertex cortical thickness with increasing PCC PiB retention controlling for age in CN subjects: vertex cluster-wise statistics determined by Monte Carlo simulation**

Cortex	X*	Y	Z	max p	Area** (mm <sup>2</sup> )	CWP***
Middle temporal, left	-58	-12	-20	0.00002	1739	0.075
Inferior parietal, left	-30	-65	40	0.00037	3617	0.0002
Supra marginal, left	-42	-46	38	0.00032	3627	0.0002
Rostral middle frontal, left	-41	35	19	0.0060	2850	0.0028
Precuneus, right	5	-57	22	0.000026	8256	0.00020
Supra marginal, right	42	-36	36	0.000013	2106	0.031
Rostral middle frontal, right	24	45	27	0.0019	3634	0.0012
Superior temporal, right	46	-36	8	0.0021	3146	0.0024

\*Talairach coordinates of vertex in cluster with maximum p-value

\*\*Surface area of cluster in standardized cortical surface

\*\*\*Cluster-wise p-value

Figures:

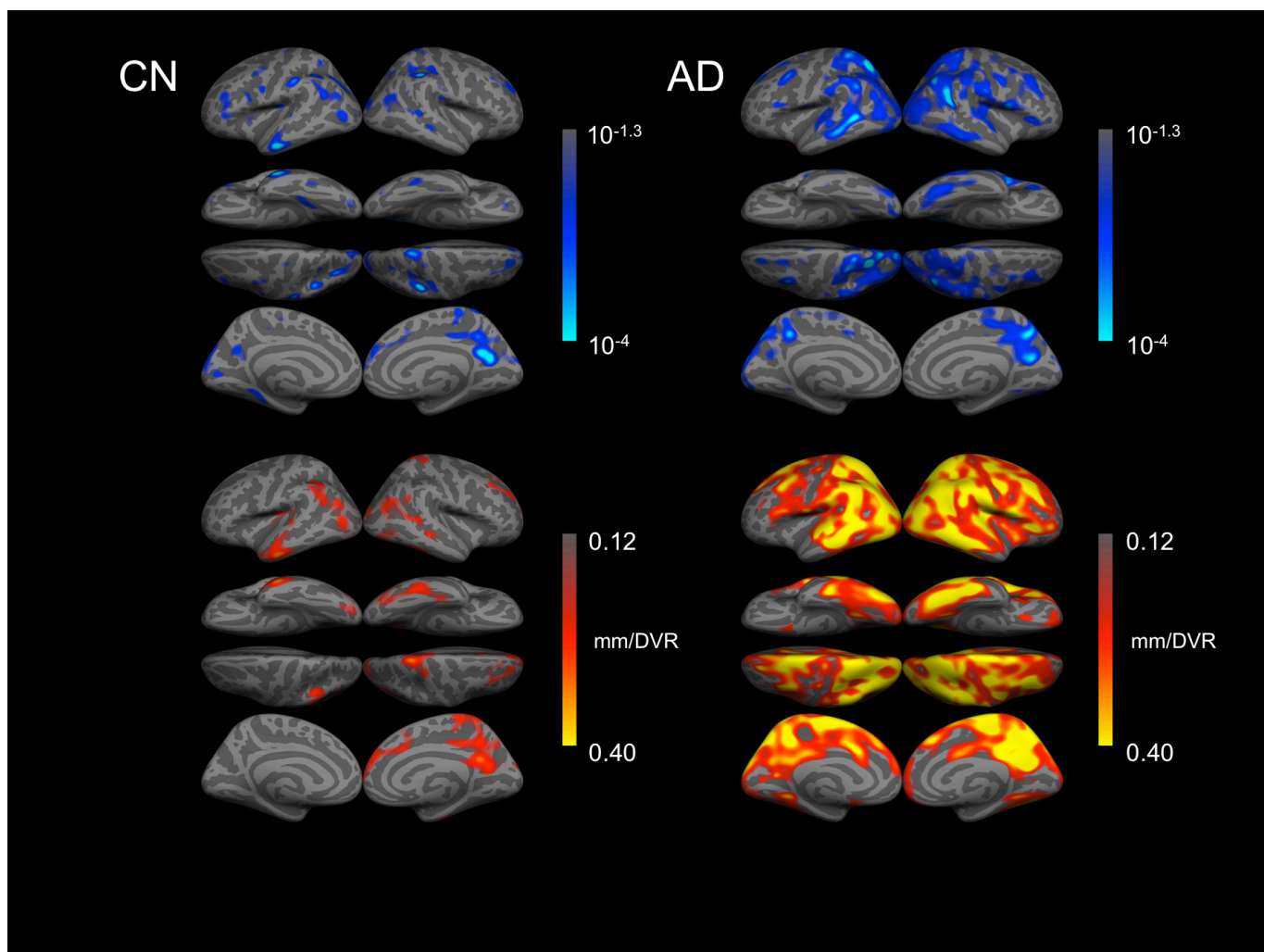


**Figure 1. A $\beta$ -associated reduction in cortical thickness in CN subjects and AD patients.** Regression coefficients expressing reduction in thickness at each vertex per unit increase in PCC DVR controlling for age (bottom row), and corresponding statistical significance as p-value (top row) in CN or AD groups (left or right column, respectively). Only clusters of 3000 or more contiguous vertices with regression coefficients exceeding 0.12 mm/DVR are shown on the bottom row of surfaces.

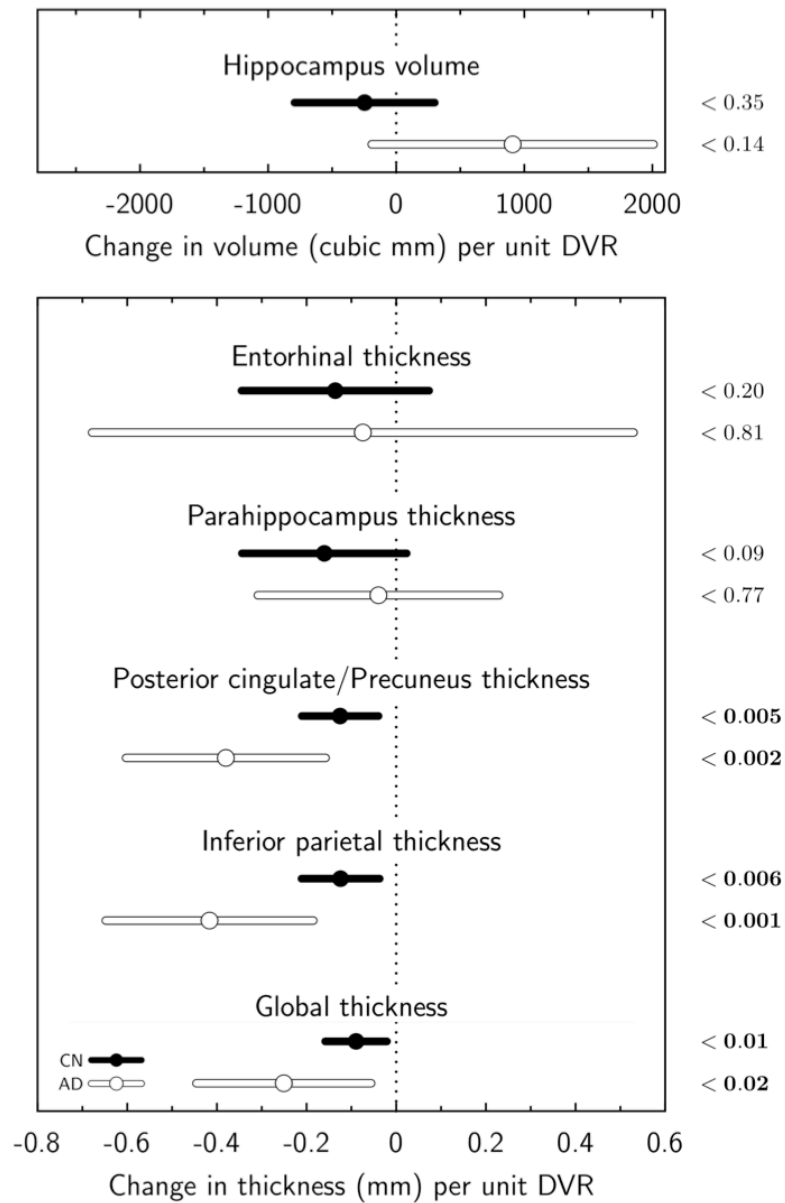


**Figure 2. A $\beta$ -associated hippocampal volume and regional thickness changes in CN and AD groups.** Regression coefficients expressing change in hippocampal volume or regional average thickness per unit increase in PCC DVR controlling for age (age and gender for hippocampal volume), and corresponding 95% confidence intervals and statistical significances (right).

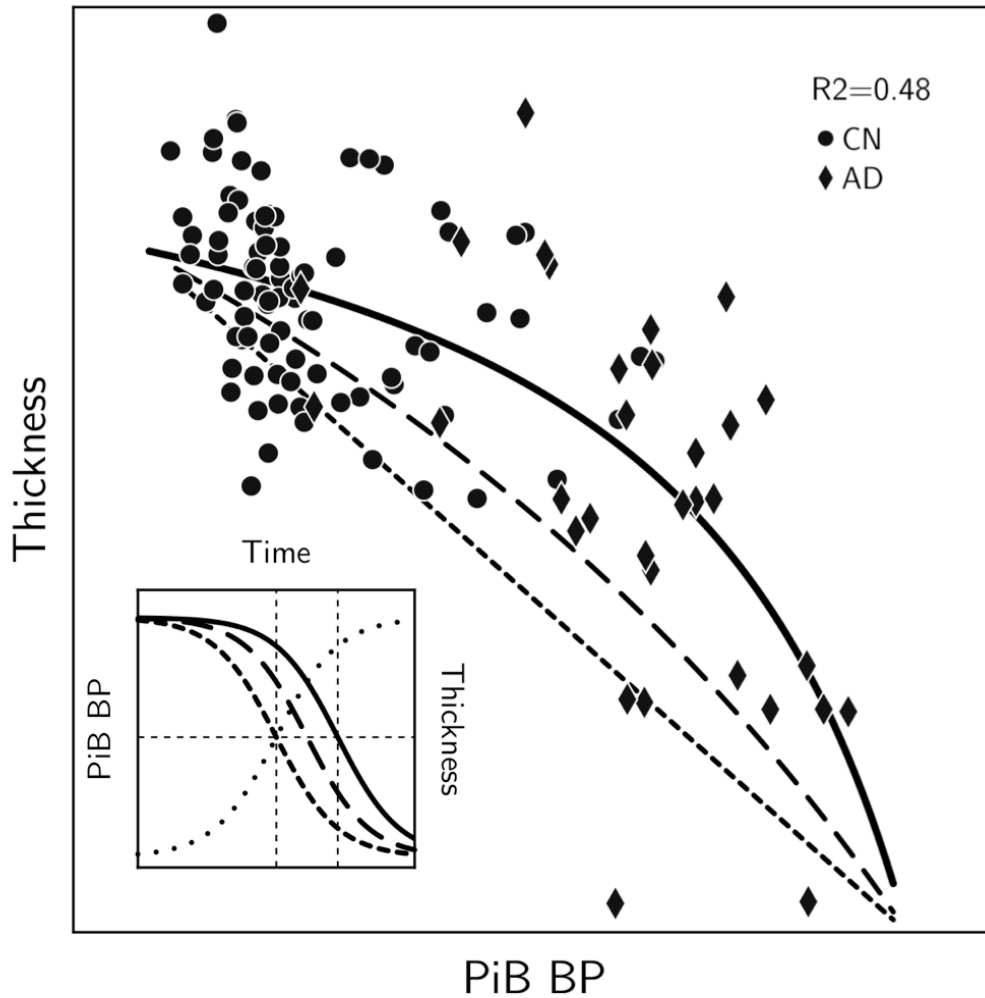


**Figure 3. Modeling of PCC thickness as a function of PiB retention in CN and AD groups.** Least squares fit (solid curve) of thickness-PiB functional relationship based on sigmoid time courses, with the maximum rate of thickness decline later in time than the maximum rate of PiB increase; compare solid (thickness) and dotted (PiB) sigmoids (inset graph). Dashed curves correspond to shorter time lags: long-dashed to one half the best-fit time lag, and short-dashed to no lag. The inset shows the underlying sigmoid time courses for PiB (dotted) and thickness at the two time lags. As the time lag between thickness and PiB increases, the curvature of the thickness-PiB curve increases. Binding potential (which is equal to DVR - 1) was used as the PiB measure in the modeling since we assumed that PiB BP asymptotes to zero prior to disease onset.